The Iron−Sulfur Clusters 2 and Ubisemiquinone Radicals of NADH:Ubiquinone Oxidoreductase Are Involved in Energy Coupling in Submitochondrial Particles†

Ronald van Belzen,‡ Alexander B. Kotlyar,§ Namdoo Moon,|| W. Richard Dunham,|| and Simon P. J. Albracht*,‡

E. C. Slater Institute, Biochemistry/FS, University of Amsterdam, Plantage Muidergracht 12, NL-1018 TV Amsterdam, The Netherlands, Department of Biochemistry, George S. Wise Faculty of Life Sciences, Ramat Aviv, 69978, Tel Aviv, Israel, and Biophysics Research Division, University of Michigan, 930 North University, Ann Arbor, Michigan 48109-1055

Received June 3, 1996; Revised Manuscript Received November 13, 1996⊗

ABSTRACT: The behavior of ubisemiquinone radicals and the iron−sulfur clusters 2 of NADH:ubiquinone oxidoreductase (Complex I) in coupled and uncoupled submitochondrial particles (SMP), oxidizing either NADH or succinate under steady-state conditions, was studied. Multifrequency EPR spectra revealed that the two new g_z lines of the clusters 2, only observed during coupled electron transfer under conditions where energy dissipation is rate-limiting [De Jong, A. M. Ph., Kotlyar, A. B., & Albracht, S. P. J. (1994) *Biochim. Biophys. Acta 1186*, 163−171], are the result of a spin−spin interaction of 2.8 mT. Investigation of the radical signals present in coupled SMP indicated that more than 90% of the radicals can be ascribed to two types of semiquinones which are bound to Complex I (Q_I-radicals) or ubiquinol:cytochrome *c* oxidoreductase (Complex III; Q_{III}-radicals). The presence of Q_{III}-radicals, but not that of Q_I-radicals, was completely abolished by uncoupler. Part of the Q_I-radicals weakly interact with the clusters 2 of Complex I. This uncoupler-sensitive interaction can amount to a splitting of the radical EPR signal of at most 1 mT, considerably weaker than the 2.8 mT splitting of the g_z lines of the clusters 2. We propose that the 2.8 mT splitting of these g_z lines results from an energy-induced spin−spin interaction between the two clusters 2 within the TYKY subunit of Complex I. The two clusters 2 show no interaction during electron transfer in uncoupled SMP or in fully-reduced anaerobic-coupled SMP. The results point to a direct role of the Fe-S clusters 2 and the Q_I-radicals in the mechanism of coupled electron transfer catalyzed by Complex I.

NADH:Q oxidoreductase[1] (EC 1.6.99.3; Complex I) isolated from bovine heart mitochondria consists of at least 41 polypeptides (molecular mass 907 kDa; Walker, 1992; Walker et al., 1992, 1995; Fearnley & Walker, 1992). The enzyme catalyzes the oxidation of NADH and the transfer of two electrons to ubiquinone. This transfer is coupled to vectorial proton translocation with a $H^+/2e^-$ stoichiometry of 4−5 (Walker, 1992; Ragan, 1987). The electron carriers involved are FMN, [2Fe-2S] clusters (1a and 1b), and [4Fe-4S] clusters (2, 3, and 4) (Albracht & Subramanian, 1977; Salerno et al., 1977). The clusters 1b and 2−4 are completely reduced within 5 ms after mixing with NADH (Orme-Johnson et al., 1974). Studies on the quantification of the Fe-S EPR signals (Albracht et al., 1977; 1979; Van Belzen et al., 1992) and on the actions of the substrate NADPH (Van Belzen & Albracht, 1989) and the inhibitor piericidine A (Van Belzen et al., 1990) support the view (Albracht, 1982; Van Belzen & Albracht, 1989; Van Belzen et al., 1990) that the minimal functional unit of Complex I comprises two of the clusters 2, 3, and 4 and only one cluster 1b.

For Complex I from *Neurospora crassa* (Weiss et al., 1991), an L-shaped structure has been recognized with electron microscopy (Hofhaus et al., 1991). Earlier studies of two−dimensional membrane crystals showed that this complex extends across the inner-mitochondrial membrane and protrudes extensively into the matrix space (Leonard et al., 1987). The peripheral domain contains most of the redox groups, namely, FMN and the Fe-S clusters 1, 3, and 4 (Wang et al., 1991). There are two pathways of protein assembly, independently leading to the two major parts of the complex, the hydrophilic peripheral domain and the hydrophobic membrane domain, which then combine to form Complex I (Friedrich et al., 1989; Wang et al., 1991; Weiss et al., 1991).

The mechanism of coupling of electron transfer to proton translocation in Complex I remains elusive. Redox-potential gaps between FMN and the isopotential clusters 1b, 3, and 4, between these clusters and the clusters 2, and between the clusters 2 and ubiquinone might all accommodate energy transduction (Weiss et al., 1991; Walker, 1992). The subunits involved in the peripheral domain show a large sequence homology to some subunits from [NiFe]- and [Fe]-hydrogenases, enzymes which contain no proton-translocating capability (Pilkington et al., 1991; Weiss et al., 1991; Walker, 1992; Albracht, 1994; Albracht & De Jong, 1996). This, and the location of this domain outside the mitochondrial membrane, makes it less likely that a proton translocation site is present here.

One of the mechanisms for proton translocation might involve the reduction of ubiquinone by Complex I. Burbaev

† This work was supported by EU Grant BIO2-CT93-0364. A.B.K. acknowledges the Netherlands Organization for Scientific Research (NWO) for a grant enabling the stay in Amsterdam.

‡ University of Amsterdam.

§ George S. Wise Faculty of Life Sciences.

|| University of Michigan.

⊗ Abstract published in *Advance ACS Abstracts,* January 1, 1997.

[1] Abbreviations: EPR, electron paramagnetic resonance; Q, ubiquinone; SMP, submitochondrial particles.

S0006-2960(96)01298-6 CCC: $14.00

et al. (1989) and Kotlyar et al. (1989) first showed that ubisemiquinones are involved in this reaction and that the amount of these radicals is apparently influenced by energy coupling. De Jong et al. (1994) confirmed this observation, but found that the formation of ubisemiquinones is an obligatory step in electron transfer from Complex I to ubiquinone and that coupling affects the spin-relaxation rate of the ubisemiquinones only (De Jong & Albracht, 1994). De Jong et al. (1994) also reported an effect of the coupling phenomenon on the EPR spectrum of the iron−sulfur clusters 2 of Complex I. During steady-state oxidation of NADH by coupled SMP, the g_z lines of these clusters seem to disappear from the spectrum, and two new lines appear with apparent *g*-values of 2.063 and 2.044 (X-band). This was the first indication of energy-induced structural changes in NADH:Q oxidoreductase. These results have been confirmed by Vinogradov et al. (1995), who proposed that the two new lines arise from a spin−spin interaction of cluster 2 with ubisemiquinone.

Here we report on more detailed investigations of the effects of the coupling phenomenon upon ubisemiquinones and the iron−sulfur clusters 2. The results indicate that energy-induced changes in the EPR line shape of the clusters 2 are due to a mutual, uncoupler-sensitive exchange interaction between the two clusters. The interaction with ubisemiquinones is much weaker. A preliminary account of this work has been given on a recent symposium (De Jong et al., 1995).

MATERIALS AND METHODS

NADH, NADPH, and NAD^+ were obtained in the purest form available from Boehringer (Mannheim). Gramicidin D was purchased from Sigma (USA). All other chemicals were of analytical grade.

Coupled submitochondrial particles were prepared, treated with oligomycin (0.5 μg/mg of protein) for optimal coupling, and activated with 1 mM NADPH under oxygen at room temperature as described earlier (Burbaev et al., 1989). Succinate dehydrogenase was activated with malonate (Burbaev et al., 1989) which was also present during the column filtration. The active SMP were stored in liquid nitrogen until use. The particles thus prepared were capable of ATP-independent succinate-driven reverse electron transfer. The enzyme activities were determined as described earlier (De Jong et al., 1994) and compared well to the activities reported elsewhere (Kotlyar & Vinogradov, 1990). The respiratory control (RC), calculated as the ratio between the rates of NADH oxidation after and before the addition of gramicidin, was 5 or more for all preparations used in this report. Reversible inactivation of the NADH dehydrogenase was established by incubating the active SMP at 37 °C for 10 min as described before (Kotlyar & Vinogradov, 1990).

Protein concentrations were determined with the biuret reaction (Gornall et al., 1949). Submitochondrial particles at a protein concentration of 40−45 mg/mL in 0.25 M sucrose, 50 mM Hepes/KOH, pH 7.6, were brought into EPR tubes cooled on ice. To delay the onset of anaerobiosis during the experiments, the oxygen concentration in the suspension of SMP was increased by gassing the EPR tubes with pure oxygen for at least 10 min. The SMP were then incubated for 10 s at 30 °C whereafter substrate was added immediately. After mixing for a few seconds (specified in the experiments), the EPR tube was rapidly immersed in cold isopentane (133 K).

X-band (9.4 GHz) EPR spectra were obtained with a Bruker ECS106 EPR spectrometer, equipped with an Oxford Instruments ESR900 helium flow cryostat with an ITC4 temperature controller. The frequency was measured with a HP 5350B Microwave Frequency Counter. The field-modulation frequency was 100 kHz. Q-band (34.5 GHz) EPR spectra were obtained with a Varian E-9 EPR spectrometer in combination with the Varian E-110 microwave bridge and the E-266 room-temperature cavity. The field-modulation frequency was 10 kHz. Cooling at Q-band was as described (Albracht, 1974). The magnetic field in Q-band and X-band was calibrated with an AEG Magnetic Field Meter. P-band (15.26 GHz) EPR measurements were obtained with a homemade EPR spectrometer, equipped with a homemade gas-flow type helium transfer tube to obtain cryogenic temperatures. The frequency was measured with a HP 5340A Microwave Frequency Counter. The magnetic field was measured by a Systron Donner Model 3193 Digital NMR Gaussmeter. The field-modulation frequency was 100 kHz.

Spectra were simulated as described (Beinert & Albracht, 1982). Ubisemiquinone concentrations were determined by direct double integration of experimental spectra recorded at 40 K with a microwave power of 2 μW and a modulation amplitude of 1.27 mT. The concentration of the clusters 2 was determined from direct double integration of the low-field half of the g_z line recorded at 16 K with a microwave power of 2 mW and a modulation amplitude of 0.63 mT. A copper standard (10 mM $CuSO_4 \cdot 5H_2O$, 2 M $NaClO_4$, 10 mM HCl) was used as a reference. Reduction of cluster 1b was determined by comparing the EPR spectra at 45 K and 2 mW with the signal of a sample completely reduced with NADH. Reduction of the clusters 3 and 4 was determined by comparing the amplitudes of the $g = 1.86$ and $g = 1.88$ troughs at 8 K and 12.8 mW, respectively, with those of an NADH-reduced preparation.

RESULTS

Three kinds of steady-state reactions were investigated in coupled and uncoupled SMP: the steady-state oxidation of NADH in activated SMP, of succinate in activated SMP, and of succinate in inactivated SMP. To verify whether the SMP were really frozen during steady-state electron-transfer conditions, the EPR signals at $g = 3$ of cytochrome *a* and $g = 6$ of cytochrome a_3 of cytochrome *c* oxidase of all samples were compared to the signals of oxidized SMP (Figure 1C, trace e). Samples in which the amplitude of the $g = 3$ line decreased by 20% or more and where the $g = 6$ line was increased (e.g., Figure 1C, trace c) were considered to be close to anaerobiosis and hence not in a true steady state. By saturating the suspension with pure oxygen before the addition of substrate, the time span of steady-state electron transfer could be extended sufficiently in all cases.

Steady-State Oxidation of NADH. The data obtained from the steady-state oxidation of NADH by coupled and uncoupled SMP were as reported previously (De Jong et al., 1994; 1995), but the effects were more pronounced and allowed us to perform a more detailed analysis. In Figure 1, all of the reported effects of coupling upon the EPR signals in SMP are present. These are the following: an apparent decrease in amplitude of the radical signal upon addition of uncoupler (Figure 1A, compare traces a and b); a difference in the line shape in the g_z region (at 2.05) of the clusters 2

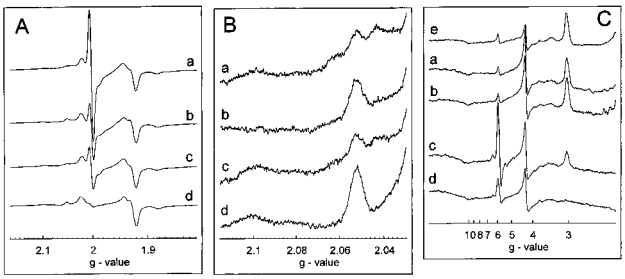

FIGURE 1: EPR spectra of coupled submitochondrial particles during NADH oxidation. (a) Oxygen-saturated SMP were mixed with 10 mM NADH (final concentration) and frozen after 5 s. (b) As (a), but now in the presence of 40 μM gramicidin. The sample was frozen 2 s after mixing. (c) Air-saturated SMP were mixed with 10 mM NADH (final concentration) and frozen after 5 s. (d) As (a), but now 40 μM gramicidin was present and the sample was frozen 5 s after mixing. (e) No substrate added. EPR conditions (A and B): microwave frequency, 9420 MHz; microwave power incident to the cavity, 2 mW; modulation amplitude, 0.64 mT; temperature, 16 K. EPR conditions (C): microwave frequency, 9420 MHz; microwave power, 12.6 mW; modulation amplitude, 1.27 mT; temperature, 11 K.

between coupled and uncoupled SMP (Figure 1B, compare traces a and b); and an additional broad signal in the region of $g = 1.93-1.96$ in coupled SMP (Figure 1A, compare traces a and b). Spin quantification revealed that the amount of radicals in different samples of coupled SMP ranged from 1.3 to 1.4 times the amount of reduced clusters 2 of Complex I, while in uncoupled SMP samples the amount of radical was equal (0.95−1.03 times) to the amount of clusters 2. The power-saturation behavior at 40 K of the radical signals in coupled and uncoupled SMP during NADH oxidation was clearly different (not shown). The differences were comparable to the saturation behavior of radicals present during pre-steady-state NADH oxidation (De Jong et al., 1995).

The samples a and b were both trapped during the steady state, since the amplitudes of the EPR signals at $g = 3$ and $g = 6$ (Figure 1C, traces a and b) were the same as those of oxidized SMP (Figure 1C, trace e). Sample c differed from sample a in that no flushing with pure oxygen was performed before the addition of NADH. This resulted in partial reduction of cytochrome *c* oxidase as judged from the increase of the line at $g = 6$ and the 50% decrease of the line at $g = 3$ (Figure 1C, trace c). The line shape in the g_z region of the clusters 2 was still that of coupled SMP (Figure 1B, trace c). The power-saturation behavior of the radicals in this sample nearly resembled the behavior of the radicals in coupled SMP during steady-state NADH oxidation (not shown). Spin quantification revealed, however, that the radical concentration in this sample had decreased to 0.90−0.95 times the concentration of the clusters 2. If gramicidin was present as well, then complete anaerobiosis was obtained within 5 s (Figure 1C, trace d), resulting in a total loss of the radical signal [Figure 1A, trace d; in accordance with Burbaev et al., (1989) and Kotlyar et al. (1989)] and a normal g_z line of the clusters 2 (Figure 1B, trace d). The results demonstrate the advantage of the use of oxygen saturation to obtain samples trapped in the steady state.

Steady-State Oxidation of Succinate. Figure 2 shows the spectra of coupled and uncoupled SMP during succinate oxidation. There is a clear difference in line shape in the $g = 1.93-1.96$ region between inactivated coupled SMP and inactivated uncoupled SMP (Figure 2A, traces b and d). Since inactivated Complex I is not reduced by reverse electron transfer, this indicates that the extra broad feature around g

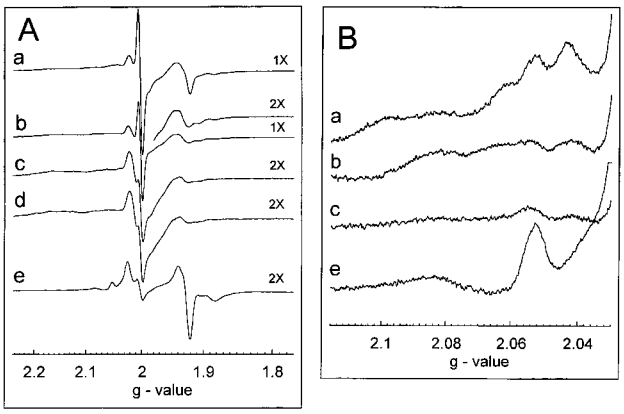

FIGURE 2: EPR spectra of coupled submitochondrial particles during succinate oxidation. (a) Oxygen-saturated SMP were mixed with 20 mM succinate (final concentration) and frozen after 6 s. (b) As (a) but now Complex I in the SMP was first inactivated. (c) As (a) but in the presence of 40 μM gramicidin. The sample was frozen 3 s after mixing. (d) As (b) but with 40 μM gramicidin present. The sample was frozen 3 s after mixing. (e) As (a) but now the sample was frozen 2 min after mixing. EPR conditions: microwave frequency, 9420 MHz; microwave power, 2 mW; modulation amplitude, 0.64 mT; temperature, 16 K.

$= 1.945$ in trace b, which is similar to that observed in activated coupled SMP during NADH oxidation (Figure 1A, trace a), is presumably not caused by an Fe-S cluster of Complex I. The difference could be observed in EPR spectra up to 77 K, suggesting the extra features to be due to a [2Fe-2S] cluster.

The lines at $g = 2.062$ and $g = 2.044$ are more pronounced in the case of succinate oxidation than in the case of NADH oxidation, using the same batch of SMP. The degree of reduction of the clusters 2 during succinate oxidation, however, was never complete (about 80% of the amount reduced by NADH). Iron−sulfur clusters 3 and 4 were reduced slightly less (about 65%), while cluster 1b was never more than 5% reduced. Prolonged incubation of coupled activated SMP with succinate (1−15 min) lowered the amount of reduced clusters 2 to 50−55%, while reduction of clusters 3 and 4 diminished to about 10%. No reduction of the Fe-S clusters of Complex I occurred in inactivated SMP or in the presence the uncoupler gramicidin (Figure 2).

Figure 3 shows the power-saturation behavior of the radicals at 40 K in SMP during succinate oxidation. The difference of the amount of radicals between activated and inactivated coupled SMP was 1.1 times the amount of clusters 2 of Complex I reducible by succinate oxidation-induced reversed electron transfer. These radicals are ascribed to ubisemiquinones bound to Complex I and will be indicated as Q_I-radicals. The total amount of radicals in activated coupled SMP was almost double this amount (1.9 times the amount of reduced clusters 2). A small amount of radical (0.13 times the amount of succinate-reducible clusters 2 in coupled particles) was present in both activated and inactivated SMP in the presence of gramicidin. The power of half-saturation of this latter radical was 12.5 mW at 40 K. The uncoupler-sensitive radicals observed in inactivated SMP are tentatively ascribed to Complex III ($P_{1/2} = 2.6$ mW at 40 K) and will be indicated as Q_{III}-radicals.

The temperature dependence of the amplitude of the succinate-induced radical signals in coupled SMP is shown in Figure 4. The temperature dependence of radicals in inactivated coupled SMP virtually followed Curie's law. The

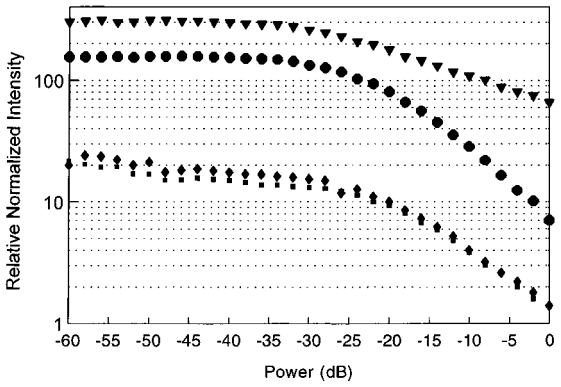

FIGURE 3: Microwave power dependence of the radical EPR signals during succinate oxidation in the absence and presence of uncoupler. The same samples as in Figure 2 were used. Inverted triangles, activated SMP (Figure 2, trace a); circles, inactivated SMP (Figure 2, trace b); diamonds, activated SMP in the presence of gramicidin (Figure 2, trace c); squares, inactivated SMP in the presence of gramicidin (Figure 2, trace d). On the logarithmic *y*-axis, the radical intensity (double-integrated spectrum), normalized for differences in microwave power and receiver gain, is plotted. EPR conditions: microwave frequency, 9420 MHz; maximum microwave power, 203 mW (0 dB); modulation amplitude, 0.64 mT; temperature, 40 K.

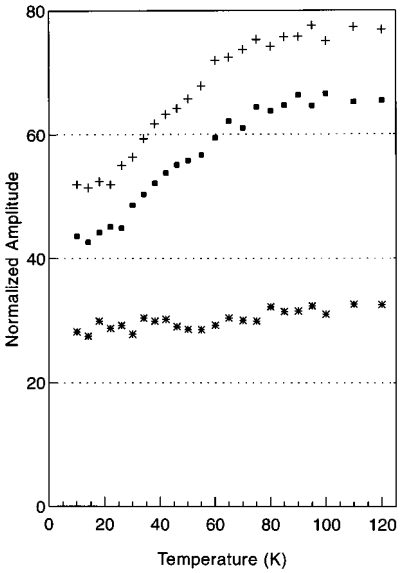

FIGURE 4: Temperature dependence of the radical EPR signals present during succinate oxidation in activated and inactivated submitochondrial particles. Coupled SMP (45 mg/mL protein) were mixed with 20 mM succinate (final concentration). In one case, the SMP were incubated 10 min at 37 °C to inactivate Complex I, prior to the addition of substrate. The samples were frozen a few seconds after mixing as indicated. Plus signs, activated SMP, frozen after 8 s; squares, activated SMP, frozen after 4 s; stars, inactivated SMP, frozen after 4 s. On the *y*-axis, the signal amplitude, normalized for differences in microwave power, receiver gain, and temperature, is plotted. EPR conditions: microwave frequency, 9420 MHz; microwave power between 200 nW and 2 μW (nonsaturating); modulation amplitude, 1.27 mT.

amplitude of the signal at 10 K is 87% of the amplitude at 120 K, while the signal intensity (double integration) remained constant. The slight decrease of the signal amplitude was accompanied by a line-width broadening from 0.91 mT at 100 K to 0.98 mT at 16 K (not shown). The *g*-value for this Q_{III}-radical was 2.0042 in X-band.

The temperature dependence of the amplitude of the radicals in activated SMP strongly deviated from Curie's law. Upon lowering the temperature, the amplitude remained constant between 120 and 75 K, decreased between 75 and

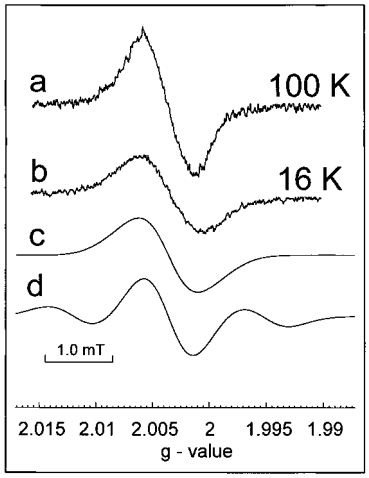

FIGURE 5: EPR spectra of Q_I-radicals in SMP during succinate oxidation. The EPR spectra of two samples as described in Figure 4 (activated SMP, 8 s; and inactivated SMP, 4 s) were both recorded at two different temperatures. The differences of the EPR spectra of activated SMP minus inactivated SMP at both temperatures are displayed. Two EPR simulations created to better understand the line shape of the 16 K difference spectrum are also displayed. (a) Difference of EPR spectra recorded at 100 K. (b) Difference of EPR spectra recorded at 16 K. (c) Addition of two isotropic EPR simulations both with $g = 2.0045$ (width = 0.75 mT) one of which (representing 35% of the total intensity) has a 2-fold splitting of 1.0 mT. (d) Addition of two isotropic EPR simulations both with $g = 2.0045$ (width = 0.75 mT) one of which (representing 35% of the total intensity) has a 2-fold splitting of 2.8 mT. EPR conditions: microwave frequency, 9420 MHz; microwave power, 200 nW at 16 K and 2 μW at 100 K; modulation amplitude, 0.25 mT; temperatures, 16 and 100 K.

22 K, and became constant again between 22 and 10 K. The intensity, obtained after double integration, remained the same between 120 and 10 K. The decrease of the signal amplitude was accompanied by an apparent line-width broadening from 0.75 mT at 100 K to 0.94 mT at 16 K for the Q_I-radicals (Figure 5). The *g*-value for this radical was 2.0047 in X-band. The increase of the (nonsaturated) line width upon lowering the temperature is ascribed to a magnetic interaction with another paramagnet, that weakly splits up (part of) the original radical signals. Figure 5, trace c, shows an attempt to simulate the radical signal measured at 16 K, with the line shape of the radical as observed at 100 K. A good fit was obtained by assuming that only 35% of all radicals were split by another $S = {}^1/_2$ system with an interaction of no more than 1.0 mT. In Figure 5, trace d, the same simulation is shown assuming a splitting of 2.8 mT. In this case, clear side bands can be detected. The temperature dependence of the amplitude of the radicals in SMP during steady-state NADH oxidation in the presence of gramicidin did not deviate from Curie's law (not shown). The line width of the radical signal under these conditions was 0.84 mT at 100 K and 0.87 mT at 16 K in X-band.

Figure 6 shows the power saturation at 22 and 100 K of the difference in signal intensity (double integration) between activated and inactivated coupled SMP during succinate oxidation. In both cases, two radicals could be identified having different power-saturation behavior. At 22 K, the intensity of the EPR signal of the radicals remained constant between −60 and −48 dB. At powers above −48 dB the signal intensity decreased as a result of power saturation. A small plateau where the signal intensity remains constant was reached around −24 dB (see arrow), which means that the signal that started to saturate at −48 dB was completely

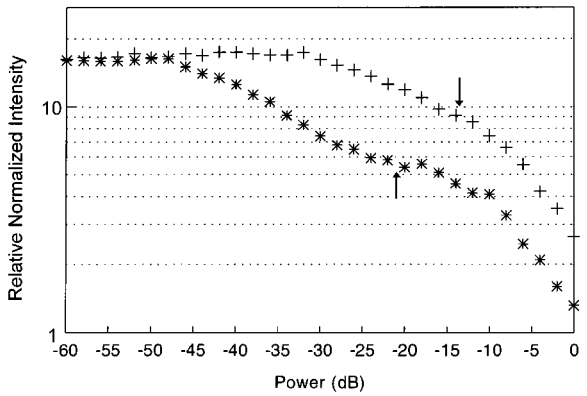

FIGURE 6: Microwave power dependence of the radical EPR signal difference between activated and inactivated SMP during succinate oxidation. The difference of the double-integrated radical intensity observed in activated and inactivated SMP is shown on a logarithmic *y*-scale. The samples are the same as described in Figure 4. Stars, activated SMP, 8 s minus inactivated SMP, 4 s recorded at 22 K; plus signs, activated SMP, 8 s minus inactivated SMP, 4 s recorded at 100 K. The arrows indicate the regions where one of the radicals becomes virtually completely saturated. EPR conditions: microwave frequency, 9420 MHz; maximum microwave power, 203 mW at 0 dB; modulation amplitude, 0.64 mT.

saturated at this power. This radical is called the slow-relaxing Q_I-radical ($P_{1/2}$ = 50 μW at 22 K), because it saturates at a relatively low power. Above the power of −18 dB, the signal intensity decreases again as a result of the saturation of a second radical, which is called the fast-relaxing Q_I-radical ($P_{1/2}$ = 120 mW at 22 K). The amount of fast-relaxing Q_I-radicals relative to the total amount of Q_I-radicals was calculated to be 35% in this particular sample. The total amount of Q_I-radical was calculated to be 95% of the amount of clusters 2 reducible by succinate oxidation-induced reversed electron transfer. In other samples, the total amount of slow- plus fast-relaxing Q_I-radicals ranged between 90% and 100% of the amount of succinate-reducible clusters 2. The amount of fast relaxing Q_I-radicals varied depending on the conditions, but never exceeded 35%.

Also at 40 K the slow-relaxing Q_I-radicals ($P_{1/2}$ = 120 μW) are separated in the power-dependence plot from the fast-relaxing Q_I-radicals by a plateau (not shown). The power of half-saturation of this latter radical, however, was so high at this temperature that we were unable to determine it ($P_{1/2}$ > 500 mW). At 100 K, the power saturation of the two Q_I-radicals can still be recognized (Figure 6), though not as clearly. It can be seen that the decrease in intensity starts at −32 dB and is linear when plotted logarithmically. Above the power of −12 dB (see arrow), the descent of the radical intensity per dB increases, which indicates the involvement of another radical. Although two Q_I-radicals can still be distinguished from this plot, they both show a considerably faster relaxation at this temperature. The power of half-saturation of the Q_{III}-radical was 3.5 mW at 100 K and 0.8 mW at 22 K, and, as already mentioned, it was 2.6 mW at 40 K.

Anisotropy of the Radical Signals. Although the EPR signals of the radicals in X-band had an isotropic appearance, anisotropy was observed in 35 GHz spectra. In Figure 7, the Q-band spectra of radicals in four different samples are displayed. Since the Q_{III}-radicals are uncoupler-sensitive, the signal in Figure 7, trace a, is ascribed to Q_I-radicals. The signal in trace d is due to Q_{III}-radicals, since Complex I-inactivated SMP were used here. The conditions used to create the signals in traces b and c imply that these signals

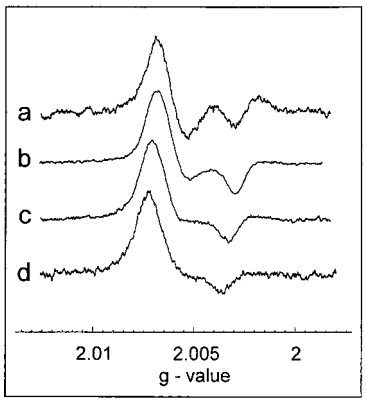

FIGURE 7: Q-band EPR spectra of radicals in coupled submitochondrial particles during NADH and succinate oxidation. Coupled SMP (45 mg/mL protein) were mixed with 10 mM NADH (final concentration) or 20 mM succinate (final concentration). In one sample, 40 μM gramicidin was added. Another sample was incubated 10 min at 37 °C to inactivate Complex I, prior to the addition of substrate. The samples were frozen after mixing at the time intervals indicated. (a) NADH, gramicidin, 3 s, 15 mg/mL protein concentration of SMP. (b) NADH, 5 s. (c) Succinate, 5 s. (d) Succinate, 5 s, inactivated. EPR conditions: microwave frequency, 34 680 MHz; microwave power, 200 μW; modulation amplitude, 1.0 mT; temperature, 80 K. The spectra were averages of 100 scans, except for the spectrum in trace a that was an average of 200 scans. The magnetic field was determined with an accuracy of ±0.2 mT.

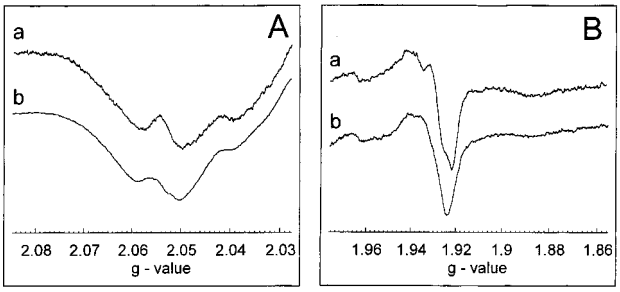

FIGURE 8: Q-band EPR spectra of the clusters 2 in coupled and uncoupled submitochondrial particles during NADH oxidation. Coupled SMP were mixed with substrate to a final concentration of 10 mM NADH. The samples were frozen after 1 min (trace a) or 5 s (trace b). EPR conditions: microwave frequency, 34 820 MHz; microwave power, 2 mW; modulation amplitude, 1.25 mT; temperature, 18 K. Trace a in panel A is an average of 100 scans, and trace b is an average of 250 scans, while traces a and b in panel B are avarages of 60 scans.

are mixtures of these two radicals. Both the Q_I- and the Q_{III}-radical signals are anisotropic. The field distances between the low-field top and high-field trough are 2.35 mT in trace a, 2.41 mT in trace b, 2.42 mT in trace c and 2.25 mT in trace d.

Analysis of the Line Shapes of the Clusters 2. In Figure 8, the line shapes of the clusters 2 as measured in Q-band are shown. The spectrum of the SMP incubated for 1 min with NADH (trace a) displays a slightly-rhombic line shape ($g_{x,y,z}$ = 1.922, 1.928, and 2.0545). The spectrum of the coupled SMP during steady-state NADH oxidation is different. The apparent positions of the lines seem to have slightly shifted, and the g_z line broadened leading to a decrease in amplitude. The sloping background and other signals in the g = 2.03−2.07 region made it difficult, however, to analyze the g_z line in detail. We have therefore also recorded spectra at P-band (15 GHz). Comparison of the g_z lines of the Fe-S clusters 2 in X-band and P-band gave the same distance (2.8 mT) between the two new lines, that appear in coupled SMP during steady-state NADH and

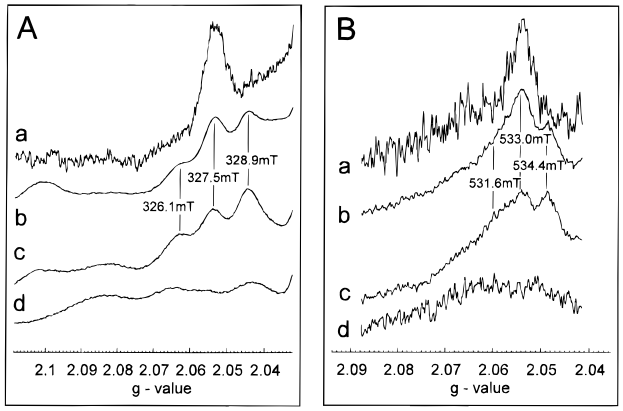

FIGURE 9: Comparison of the g_z region of the clusters 2 in X-band and P-band. Coupled SMP (45 mg/mL protein) were mixed with 10 mM NADH (final concentration) or 20 mM succinate (final concentration). In one sample, 40 μM gramicidin was added. Another sample was incubated 10 min at 37 °C to inactivate Complex I, prior to the addition of substrate. The samples were frozen after mixing at the time intervals indicated. (a) NADH, gramicidin, 3 s, 15 mg/mL protein concentration of SMP. (b) NADH, 5 s. (c) succinate, 8 s. (d) succinate, 4 s, inactivated. (A) X-band EPR conditions: microwave frequency, 9420 MHz; microwave power, 2 mW; modulation amplitude, 0.64 mT; temperature, 16 K. (B) P-band EPR conditions: microwave frequency, 15 324 MHz; microwave power, 1 mW; temperature, 15 K. The spectra in panel B are averages of 8 scans (traces a and d), 244 scans (trace b), and 209 scans (trace c).

succinate oxidation (Figure 9). This identical separation at different microwave frequencies proves that these two lines result from a spin−spin interaction.

DISCUSSION

Assignment and Properties of the Radical EPR Signals. The EPR signals of the radicals, observed during the steady-state oxidation of NADH or succinate, might originate from ubisemiquinones stabilized by the Complexes I, II, and III, as well as from flavosemiquinones. Q_I-radicals can be discriminated from others by comparing coupled submitochondrial particles, having Complex I in the active state, with SMP containing reversibly-inactivated Complex I. Coupled SMP with active Complex I are capable of ATP-independent reverse electron transfer driven by the $\Delta\mu_{H^+}$ produced by succinate oxidation. Q_I-radicals are only formed in SMP containing active Complex I. The other components of the respiratory chain are not noticeably influenced by the procedure to inactivate Complex I (Kotlyar & Vinogradov, 1990). During the present experiments, it was noticed that coupled SMP, in which Complex I had been inactivated by incubation for 10 min at 37 °C, reached anaerobiosis slightly faster during succinate oxidation, but this was the only difference that was observed. The effect is probably due to a slight decrease of the respiratory control of these SMP by the treatment.

The Q_I-radical concentration calculated from the difference between active and inactive, coupled SMP during steady-state oxidation of succinate was stoichiometric to the amount of reduced iron−sulfur clusters 2 of Complex I under these conditions. Uncoupler almost abolished all radical signals in these SMP (Figure 3). This shows that also the radical signal formed in coupled SMP with inactive Complex I is uncoupler-sensitive. We tentatively assign this type of radical to ubisemiquinones bound to Complex III (Q_{III}). As far as we know, an uncoupler-sensitive Q_{III}-radical has not yet been reported in literature. The presence of two pH-dependent ubisemiquinone radicals associated with Complex III ($Q^{\bullet-}_{in}$ and $Q^{\bullet-}_{out}$) has been described (De Vries et al., 1980, 1981; Ohnishi & Trumpower, 1980). The line width of the Q_{III}-radical signal in X-band resembles that of $Q^{\bullet-}_{in}$, but the power of half-saturation of Q_{III} is higher than those reported for both $Q^{\bullet-}_{in}$ and $Q^{\bullet-}_{out}$ (De Vries et al. 1980). We assume that during steady-state oxidation of succinate by coupled SMP, the constant flux of protons creates a local pH increase at the outside of these SMP, leading to a stablization of $Q^{\bullet-}_{in}$; hence, we tentatively conclude that Q_{III} is $Q^{\bullet-}_{in}$.

Table 1: Survey of the Appearance of Ubisemiquinone Radicals and the Reduction of Fe-S Clusters 2

conditions	species $Q_{I,s}$	$Q_{I,f}$	Q_{III}	reduced clusters 2 (%)
active SMP[a]				
NADH	+	+[c,d]	+	100
NADH/uncoupler	+[d]	−	−	100
succinate	+	+[d]	+	80
succinate/uncoupler	−	−	−	0
inactive SMP[b]				
succinate	−	−	+	0
succinate/uncoupler	−	−	−	0

[a] SMP with active Complex I. [b] SMP with inactive Complex I. [c] Maximally 35% of total Q_I-radicals. [d] Concentration of total Q_I always equals that of reduced clusters 2.

The residual radicals (6% of the total amount in activated coupled SMP during succinate oxidation) found in the presence of uncoupler cannot be assigned. They may be due to flavin of succinate dehydrogenase and/or ubiquinone reacting with this enzyme. It may also be due to ubisemiquinones associated with Complex III that is still stabilized at pH 7.6 (Ohnishi & Trumpower, 1980; De Vries et al., 1981).

As shown in Figure 3, the formation of Q_{III}-radicals during succinate oxidation is completely sensitive to gramicidin. From this observation, it can be concluded that the radicals detected in uncoupled SMP during steady-state NADH oxidation must belong to Complex I only. The amount of Q_I-radicals found under these conditions was equivalent to the amount of the reduced clusters 2 of Complex I. Since this stoichiometry was also found in coupled SMP during steady-state succinate oxidation, this confirms earlier findings (De Jong & Albracht, 1994; De Jong et al., 1995) that the amount of Q_I-radical is not influenced by uncoupler. The stoichiometry determined in this study is higher than an earlier estimation of at least one Q_I-radical per two clusters 2 (De Jong et al., 1994). Due to better defined experimental conditions, we consider the present quantification of the Q_I-radical considerably more accurate than in our earlier work. The fact that the amount of Q_I-radical is uncoupler-insensitive is in conflict with conclusions from Vinogradov and coworkers (Vinogradov et al., 1995). However, in that report, the presence of the Q_{III}-radical was not recognized. A summary of the appearance of the three radicals is given in Table 1.

We are now able to compare the behavior of the Q_I-radical in coupled and uncoupled SMP. A most interesting observation is the decrease in amplitude of the Q_I-radical in coupled SMP between 75 and 22 K (Figure 4). This is accompanied by a line broadening of its EPR signal (Figure 5). No such effect was observed for the Q_I-radical in uncoupled SMP

during NADH oxidation. The most probable cause for this line broadening is a spin−spin interaction with a rapidly-relaxing paramagnet whose relaxation time is so short at temperatures above 22 K that thermal averaging begins to lower its effect on the radical signal. At high temperature (>75 K), the spin relaxation rate of the partner spin is so fast that the interaction is averaged out. The best candidates in Complex I to fit the temperature profile of the fast Q_I-radical observed in Figure 4 are the iron−sulfur clusters 2. Optimal sharpening of the EPR signals of the clusters 2 is obtained at 20 K and below. A weak interaction between the clusters 2 and the Q_I-radical (giving rise to an increased line width) would also explain the increased relaxation rate of the Q_I-radical at low temperatures. It remains unclear how this interaction is reflected in the EPR line shapes of the clusters 2. From Figure 6, we conclude that there are two different types of Q_I-radicals present in coupled SMP: one type whose relaxation is slow ($Q_{I,s}$) and one type whose relation is fast ($Q_{I,f}$). In uncoupled SMP oxidizing NADH, only $Q_{I,s}$-radicals are present. Figure 6 allows an estimate of the relative amount of the $Q_{I,f}$-radicals (35%). For the simulation of the overlapping $Q_{I,f}$- and $Q_{I,s}$-radicals (Figure 5, trace c), we assumed that only $Q_{I,f}$-radicals are broadened by spin−spin interaction with the clusters 2. The simulation predicts a spin−spin interaction of at most 1 mT.

With the information about the behavior of the Q_I- and Q_{III}-radicals, it is also possible to interpret the results of the sample of coupled SMP during NADH oxidation that almost reached anaerobiosis (Figure 1, trace c). This sample was prepared by mixing air-saturated SMP with NADH and freezing after 5 s. It demonstrates the importance of saturation of the SMP in the EPR tubes with pure oxygen to allow sufficient time after mixing with the substrate to freeze the samples in the true steady state. In the air-saturated sample, the Q_{III}-radicals were no longer detected. Also the relative amounts of the split g_z lines of the clusters 2 and the amount of $Q_{I,f}$-radical had decreased, while the total amount of Q_I-radicals remained stoichiometric to the amount of clusters 2. Since the sample was no longer in the steady state due to oxygen shortage (the EPR signals of the hemes in cytochrome *c* oxidase showed the sample to be no longer fully aerobic), the most likely explanation is that the $\Delta\mu_{H^+}$ had decreased. The Q_{III}-radicals, which are always present in amounts substoichiometric toward Complex III, apparently are very sensitive to the loss of $\Delta\mu_{H^+}$ and disappeared first. The behavior of the radicals in this sample is in agreement with that obtained from comparison of samples with inactivated Complex I with those with active Complex I during steady-state succinate oxidation (Figure 6). It demonstrates that the behavior of the Q_I-radical is the same both in coupled SMP during NADH oxidation and in coupled SMP during succinate oxidation-driven ATP-independent electron reversal. The line width of the Q_I-radical in this sample was 0.75 mT at 100 K in X-band and is the same as observed in coupled SMP during steady-state succinate oxidation. The line width of the radical signal in SMP during steady-state NADH oxidation in the presence of gramicidin was 0.84 mT at 100 K. This difference in line width indicates that the $Q_{I,s}$-radical is not identical in coupled and uncoupled SMP. This might reflect a difference in the environment at the binding site of the $Q_{I,s}$-radical induced by the coupling phenomenon or by the presence of gramicidin.

The Q-band EPR signals of the ubisemiquinones in SMP during steady-state NADH and succinate oxidation were all anisotropic (Figure 7). A similar anisotropy was also reported for ubisemiquinone radicals in isolated Complex I (Suzuki & King, 1983). The anisotropy was ascribed to the fact that the ubisemiquinone is immobilized when it is bound to protein. EPR spectra at 95 GHz of free semiquionone radical anions of ubiquinone-10 dissolved in isopropyl alcohol (Burghaus et al., 1993) show that the EPR spectrum is inherently rhombic (g_{xyz} = 2.0065, 2.0054, 2.0022). The Q-band spectra of the Q_I-radicals in Figure 7a have a low-field top at g = 2.007 and a high-field trough (g_z value) at 2.003. In isolated Complex I (Suzuki & King, 1983), these values were 2.006 and 2.002, respectively. We conclude that the *g*-values of ubisemiquinone are not much disturbed by binding to Complex I. Due to the lower microwave frequency (35 GHz), the Q-band spectra do not show a resolved g_{xy} region.

Microwave power-saturation behavior indicated the presence of two kinds of radicals bound to Complex I (Suzuki & King, 1983). Later a ubiquinone-binding protein was isolated from Complex I, binding 1 mol of ubiquinone/mol of protein (Suzuki & Ozawa, 1986). It should be noted that the kinetic properties of the Q_I-radicals in SMP and purified Complex I are completely different. In active SMP Q_I-radicals develop within 40 ms after mixing with NADH and disappear if electron transfer comes to a halt (De Jong & Albracht, 1994). In purified Complex I, the radicals are only optimal 5 min after addition of NADH and remain constant for up to 10 min (Suzuki & King, 1983). Anisotropy was also found for the Q_{III}-radical (Figure 7, trace d). Also for Complex III a ubiquinone-binding protein has been identified (Berden et al., 1987; Usui et al., 1990). As shown in the present report, the Q_I- and Q_{III}-radicals have completely different kinetic properties. Although both radicals only show up during steady-state electron transfer, the Q_{III}-radical is strictly dependent on coupling, whereas the Q_I-radical is not. Thus, the mechanisms of semiquinone accumulation in Complexes I and III are apparently not related.

The results on the semiquinone radicals in this report extend our previous observations (De Jong & Albracht, 1994; De Jong et al., 1994). They seem to differ significantly, however, from those reported by Vinogradov and colleagues (Vinogradov et al., 1995). Especially, the powers of half-saturation of the radicals associated with Complex I in their report seem unrelated to the values we present here. These differences might be due to differences in instrumentation, samples, or the method used to distinguish the power of half-saturation of the radicals. In addition, we found no evidence for the assumption that the 2.8 mT splitting of the g_z line of cluster 2 (Vinogradov et al., 1995; these authors do not recognize the presence of two clusters 2) results from a spin−spin interaction between Q_I-radical and iron−sulfur cluster 2. A splitting of such a magnitude will show up in the EPR spectrum of the Q_I-radicals as "wings" (Figure 5). We find no indication of such a splitting of the ubisemiquinone radicals at any temperature and microwave power. Vinogradov et al. (1995), who likewise could not detect such a splitting, explained this phenomenon by assuming that the absence of significant broadening of the observable SQ_{Nf} (=$Q_{I,f}$) signal apparently originated from very rapid relaxation of cluster 2. This would result in a significant decrease in signal intensity measured at 16 K as compared to 100 K. We did not observe such a decrease of signal intensity.

The EPR Signals of the Iron−Sulfur Clusters 2. The results from Figure 9 clearly demonstrate that the two

apparent g_z lines for the clusters 2 in coupled SMP originate from a spin−spin interaction that splits the original g_z lines at 2.054 by 2.8 mT. This spin−spin interaction is uncoupler-sensitive and is observed during both NADH and succinate oxidation by coupled SMP (Figures 1B, 2B, and 9). Replacing H_2O by D_2O did not noticeably alter the line shape of the g_z region of the clusters 2 in coupled SMP during NADH oxidation (De Jong, 1994). This excludes the possibility that the splitting is caused by a proton. One of the remaining causes for the splitting is a mutual interaction of the two clusters 2, which we believe to be both present within the TYKY subunit of Complex I. Analysis of the operon encoding Complex I in *Escherichia coli* (Weidner et al., 1993) shows that only 14 of the 41 polypeptides of the bovine mitochondrial enzyme are essential for coupled electron transfer. Five polypeptides show conservative Cys patterns that might accommodate Fe-S clusters. Four of these are quite likely inherited from hydrogenases (Albracht, 1994; Albracht & De Jong, 1996). The remaining polypeptide, the TYKY subunit, contains two Cys patterns typical for two classical cubane clusters, one of which was proposed to be Fe-S cluster 2 (Dupuis et al., 1991). We propose that the two kinetically different Fe-S clusters 2 (Van Belzen & Albracht, 1989; Van Belzen et al., 1990) are present in the TYKY subunit and are involved in a mutual spin-exchange interaction, which results in a splitting of the original g_z lines of Fe-S clusters 2. The two clusters 2 do not interact in uncoupled SMP. Interaction of the two clusters 2 in coupled SMP via a dipolar mechanism, as a result of a change in relative orientation and/or distance, might explain the data. In that case, however, a half-field EPR transition would be expected. We failed to detect a half-field transition under any condition. We therefore favor an energy-induced change of the intervening protein environment such that the clusters become electronically linked, resulting in an exchange interaction.

There is a slightly-resolved structure in the g_{xy} region of the EPR signals at Q-band of the clusters 2 in fully-reduced SMP (Figure 8B). It can be caused either by slight rhombicity of both clusters or by a small difference of the $g_\perp$ value of the clusters. We did not observe such a structure with purified Complex I. The line shape changed during coupled electron transfer, presumably as result of line broadening.

The results in this report strongly indicate that both the Q_I-radicals and the two Fe-S clusters 2 are directly involved in coupled electron transfer catalyzed by Complex I.

REFERENCES

Albracht, S. P. J. (1974) *J. Magn. Reson. 13*, 299−303.

Albracht, S. P. J. (1982) in *Flavins and Flavoproteins* (Massey, V., & Williams, C. H., Eds.) pp 759−762, Elsevier/North-Holland Inc., New York.

Albracht, S. P. J. (1994) *Biochim. Biophys. Acta 1188*, 167−204.

Albracht, S. P. J., & Subramanian, J. (1977) *Biochim. Biophys. Acta 462*, 36−48.

Albracht, S. P. J., & De Jong, A. M. P. (1996) *Biochim. Biophys. Acta* (in press).

Albracht, S. P. J., Dooijewaard, G., Leeuwerik, F. J., & van Swol, B. (1977) *Biochim. Biophys. Acta 459*, 300−317.

Albracht, S. P. J., Leeuwerik, F. J., & van Swol, B. (1979) *FEBS Lett. 104*, 197−200.

Beinert, H., & Albracht, S. P. J. (1982) *Biochim. Biophys. Acta 459*, 245−277.

Berden, J. A., van Hoek, A. N., De Vries, S., & Schoppink, P. J. (1987) in *Cytochrome systems: Molecular biology and bioenergetics* (Papa, S., Chance, B., & Ernster, L., Eds.) pp 523−531, Plenum Press, New York.

Burbaev, D. Sh., Moroz, L. A., Kotlyar, A. B., Sled, V. D., & Vinogradov, A. D. (1989) *FEBS Lett. 254*, 47−51.

Burghaus, O., Plato, M., Rohrer, M., Möbius, K., MacMillan, F., & Lubitz, W. (1993) *J. Phys. Chem. 97*, 7639−7647.

De Jong, A. M. Ph. (1994) in *Electron transfer and energy transduction in mitochondrial NADH−ubiquinone oxidoreductase* (Ph.D. Thesis), University of Amsterdam.

De Jong, A. M. Ph., & Albracht, S. P. J. (1994) *Eur. J. Biochem. 222*, 975−982.

De Jong, A. M. Ph., Kotlyar, A. B., & Albracht, S. P. J. (1994) *Biochim. Biophys. Acta 1186*, 163−171.

De Jong, A. M. Ph., Molenaar, P. J., Albracht, S. P. J., Van Belzen, R., & Kotlyar, A. B. (1995) *Protein Sci. 4, Suppl. 1*, 86.

De Vries, S., Berden, J. A., & Slater, E. C. (1980) *FEBS Lett. 122*, 143−148.

De Vries, S., Albracht, S. P. J., Berden, J. A., & Slater, E. C. (1981) *J. Biol. Chem. 256*, 11996−11998.

Dupuis, A., Skehel, J. M., & Walker, J. E. (1991) *Biochemistry 30*, 2954−2960.

Fearnley, I. M., & Walker, J. E. (1992) *Biochim. Biophys. Acta 1140*, 105−134.

Friedrich, T., Hofhaus, G., Ise, W., Nehls, U., Schmitz, B., & Weiss, H. (1989) *Eur. J. Biochem. 180*, 173−180.

Gornall, A. G., Bardawill, C. J., & David, M. M. (1949) *J. Biol. Chem. 177*, 751−766.

Hofhaus, G., Weiss, H., & Leonard, K. (1991) *J. Mol. Biol. 221*, 1027−1043.

Kotlyar, A. B., & Vinogradov, A. D. (1990) *Biochim. Biophys. Acta 1019*, 151−158.

Kotlyar, A. B., Sled, V. D., Burbaev, D. Sh., Moroz, L. A., & Vinogradov, A. D. (1989) *FEBS Lett. 264*, 17−20.

Leonard, K., Haiker, H., & Weiss, H. (1987) *J. Mol. Biol. 194*, 277−286.

Ohnishi, T. (1975) *Biochim. Biophys. Acta 387*, 475−490.

Ohnishi, T., & Trumpower, B. L. (1980) *J. Biol. Chem. 255*, 3278−3284.

Orme-Johnson, N. R., Hansen, R. E., & Beinert, H. (1974) *J. Biol. Chem. 249*, 1922−1927.

Pilkington, S. J., Skehel, J. M., Gennis, R. B., & Walker, J. E. (1991) *Biochemistry 30*, 2166−2175.

Ragan, C. I. (1987) *Curr. Top. Bioenerg. 15*, 1−36.

Salerno, J. C., Ohnishi, T., Blum, H., & Leigh, J. S. (1977) *Biochim. Biophys. Acta 494*, 191−197.

Suzuki, H., & King, T. E. (1983) *J. Biol. Chem. 258*, 352−358.

Suzuki, H., & Ozawa, T. (1986) *Biochem. Biophys. Res. Commun. 138*, 1237−1242.

Usui, S., Yu, L., & Yu, C. A. (1990) *Biochemistry 29*, 4618−4626.

Van Belzen, R., & Albracht, S. P. J. (1989) *Biochim. Biophys. Acta 974*, 311−320.

Van Belzen, R., van Gaalen, M. C. M., Cuypers, P. A., & Albracht, S. P. J. (1990) *Biochim. Biophys. Acta 1017*, 152−159.

Van Belzen, R., De Jong, A. M. Ph., & Albracht, S. P. J. (1992) *Eur. J. Biochem. 209*, 1019−1022.

Vinogradov, A. D., Sled, V. D., Burbaev, D. S., Grivennilova, V. G., Moroz, I. A., & Ohnishi, T. (1995) *FEBS Lett. 370*, 83−87.

Walker, J. E. (1992) *Q. Rev. Biophys. 25*, 253−324.

Walker, J. E., Arizmendi, J. M., Dupuis, A., Fearnley, I. M., Finel, M., Medd, S. M., Pilkington, S. J., Runswick, M. J., & Skehel, J. M. (1992) *J. Mol. Biol. 226*, 1051−1072.

Walker, J. E., Skehel, J. M., & Buchanan, S. K. (1995) *Methods Enzymol. 260*, 14−34.

Wang, D.-C., Meinhardt, S. W., Sackmann, U., Weiss, H., & Ohnishi, T. (1991) *Eur. J. Biochem. 197*, 257−264.

Weidner, U., Geier, S., Ptock, A., Friedrich, T., Leif, H., & Weiss, H. (1993) *J. Mol. Biol. 233*, 109−122.

Weiss, H., Friedrich, T., Hofhaus, G., & Preis, D. (1991) *Eur. J. Biochem. 197*, 563−576.

BI9612982